

# Modeling and Simulation of Controller for Single Phase and Three Phase PWM Rectifiers

Nagisetty Sridhar<sup>1</sup> and R. Kanagaraj<sup>2\*</sup>

<sup>1</sup>Department of Electrical and Electronics Engineering, Jerusalem College of Engineering, Chennai – 600100, Tamil Nadu, India; sridharnagisetty@yahoo.com

<sup>2</sup>Department of Electrical and Electronics Engineering, Bharath University, Chennai – 600100, Tamil Nadu, India; kanagaraj.eee@bharathuniv.ac.in

## Abstract

This paper presents the modeling of single phase, three phase rectifiers and suitable controller design for the modeled rectifier circuit the primary application of rectifiers is to derive DC power from an AC supply. Virtually all electronic devices require DC, so rectifiers are used inside the power supplies of all electronic equipment. PWM rectifier is now becoming popular due to its low distortion input current, unity power factor operation, bi-directional power flow ability and can offer excellent dynamic response of the dc output voltage. A three-phase PWM rectifier used together with closed-loop dc–dc converters for converting DC power from one voltage to another is much more complicated. In order to perform the above operation rectifier switches should be controlled properly. Hence it is much needed to design a suitable controller for single phase and three phase rectifier. From the small signal transfer function model, the controller scan be designed and the simulated results are presented.

**Keywords:** Bidirectional AC-DC Converters, Mathematical Model, PWM rectifiers

## 1. Introduction

The single-phase Voltage Source PWM Rectifier (VSR) is widely used in improving the quality of the power energy. Recently, lots of researches have been investigated for the Single-Phase PWM rectifier. The single-phase PWM rectifier is now becoming more and more popular due to its low distortion input current, unity power factor operation and bi-directional power flow ability. As the filter capacitor required is generally small under balanced supply voltage conditions, it may also be believed that these converters can offer excellent dynamic response of the dc output voltage.

In general, the selection of an appropriate controller of a PWM rectifier in consideration of stability and dynamic performances requires good knowledge about the characteristics of the system to be controlled. Various strategies have been applied on the single-phase PWM rectifier, such as states-space averaging and circuit methods.

A three-phase PWM rectifier is often used together with closed-loop dc–dc converters as loads. The three phase PWM rectifier can be compared with the working of DC-DC boost converter. SISO model can be derived for the three phase PWM rectifier so that it can be comparable with the DC-DC boost converter

In this paper, the suitable controller for small signal transfer function model for single phase PWM rectifier was designed under closed loop operation and also SISO model, controller for closed loop operation of three phase rectifier was designed.

## 2. Boost Rectifier

Single-phase PWM rectifier based on the small signal model are dealt in detail. The purpose is to decrease the voltage fluctuations and increase the dynamic performance of the rectifier when the load changes suddenly<sup>1</sup>. The procedure for deriving the transfer

\* Author for correspondence

function are to make assumptions then define the state variables and write state equations for each interval of operation, average the state equations over a switching cycle and introduce perturbation in state variables then equate ac and dc quantities and proceed with ac equations and take Laplace transform, prepare matrix Small signal model and calculate desired transfer functions

The Figure 1 shows the basic equivalent circuit of single phase PWM rectifier. Figure 2 and Figure 3 shows the mode of operation for PWM rectifier acting as a boost rectifier. PWM rectifier can be used as bidirectional rectifiers. Rectifier operation is performed by the diodes, while the inverter operation is performed by switches. As tabulated in Table 1, it can operate the rectifier in a boost mode by controlling the switches  $T_1, T_2$  with the help of the inductor at source<sup>2</sup>.

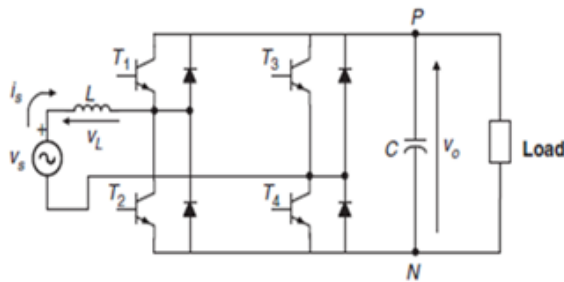


Figure 1. Single phase Boost rectifier.

Under steady state operation, mode 1, when switch  $T_2$  is ON, the conduction path is given by  $V_s-L-T_2-D_4$ . Hence the inductor is charging, since there is no connection to the load<sup>3</sup>. This mode of operation is similar to that of the DC-DC boost converter operation when switch is ON. In Mode 2, when  $T_2$  is OFF, the conduction path will be  $V_s-L-D_1-load-D_4$ . Here the inductor is discharging mode. More over the switches  $T_3$  and  $T_4$  has no effect on the operation of a boost rectifier.

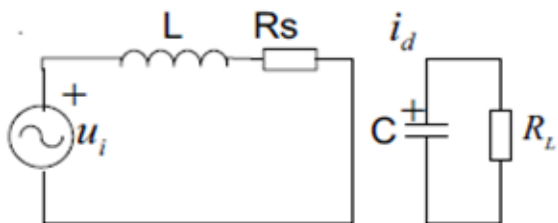


Figure 2. Mode 1/3 operation.

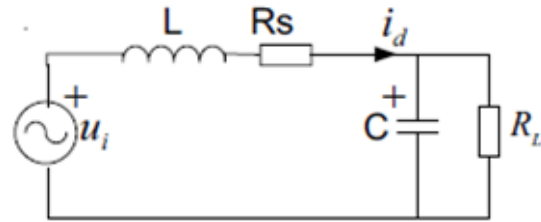


Figure 3. Mode 2/4 operation.

Table 1. Modes of operation

SUPPLY	MODE	$T_1$	$T_2$	PATH
+ <sub>ve</sub> cycle	1	OFF	ON	$V_s-L-T_2-D_4$
+ <sub>ve</sub> cycle	2	ON	OFF	$V_s-L-D_1-l-D_4$
- <sub>ve</sub> cycle	3	ON	OFF	$V_s-D_3-T_1-L$
- <sub>ve</sub> cycle	4	OFF	ON	$V_s-D_3-l-D_2-L$

### 3. Design of Converter Parameters

Inductor and capacitor will play a major role in the boost rectifier as shown in the operation. Inductance is used for bi-directional power flow and boost operation, while the capacitance is used to maintain the constant DC output for a period of time by reduce the output DC ripples<sup>4</sup>. Hence designing of inductance and capacitance have a significant role in the operation. Moreover the modulating index must be less than 1 for PWM pulse. Hence the amplitude of modulating signal must be greater than of the amplitude of carrier signal<sup>5</sup>.

#### 3.1 Voltage Gain

The boost voltage obtained in the output can be calculated by

$$V_o = V_s M.I / (1 - d) \tag{1}$$

Where, M. I = Modulating index

d = switching period

#### 3.2 Inductance

The fundamental component of PWM switch should be given by  $V_r$ . It should be varied from the supply voltage at an angle of  $\delta$  as the line is similar to that of transmission line.

The inductance can be derived as follows

$V_r$  = Fundamental component of PWM waveform  
 $V_s$  = Supply Voltage,  $I_s$  = Supply currents

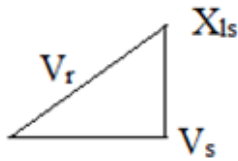


Figure 4. Phasor diagram.

$$V_r = \sqrt{V_s^2 + (L\omega I_s)^2} \tag{2}$$

From the above equation we can find L as

$$L = \sqrt{\frac{V_r^2 - V_s^2}{\omega^2 I_s^2}} \tag{3}$$

### 3.3 Capacitance

$I_L$ , the load current contains DC current and ripples current<sup>6</sup>. Capacitor makes  $I_L$  perfect DC and ripple should be maximum of 5%. By equating output power equals to input power and equate  $I_L$  with the AC part we can obtain the value of capacitance as follows

$$C \geq (MI \cdot I_s) / (4\omega \Delta V) \tag{4}$$

### 3.4 Carrier Frequency

The carrier frequency should be minimum in the order of  $11 \cdot f_s$ , where  $f_s$  is the supply or fundamental frequency<sup>7</sup>. For 50Hz supply it should be above 550Hz. Most probably 2KHz is chosen.

## 4. Small Signal Mode

Assume all of the switches are ideal time-variant switch model. Also, suppose the inductor current and the capacitor voltage is state variable<sup>8</sup>. Then we can get the math model when the switches turn on/off. The mathematical model can be calculated as

$$L \frac{di}{dt} = u_i - u_c \cdot C \frac{du_c}{dt} = i - \frac{u_c}{R} \tag{5}$$

$$L \frac{di}{dt} = u_i \cdot C \frac{du_c}{dt} = \frac{u_c}{R} \tag{6}$$

So the following equations show the ideal small signal model

$$x = \begin{bmatrix} i \\ u_c \end{bmatrix}, A_1 = \begin{bmatrix} 0 & 0 \\ 0 & 1/RC \end{bmatrix},$$

$$A_2 = \begin{bmatrix} 0 & 1/L \\ 1/C & -1/RC \end{bmatrix} B_1 = B_2 = \begin{bmatrix} 1/L \\ 0 \end{bmatrix}, u = [u_i]$$

## 4.1 Average State Equation

The first step is to use the average state function instead of the two partition state functions<sup>9</sup>. According to the proportion weighted average of the state function in on/off state, we get the state space average model in on switch period. Assume D is the average of the switch variable

$$\begin{cases} L \frac{di}{dt} = u_i - (1-D)u_c \\ C \frac{du_c}{dt} = (1-D)i + (2D-1)u_c/R \end{cases} \tag{7}$$

The state-space average mode can be depicted as that

$$\begin{bmatrix} \frac{di}{dt} \\ \frac{du_c}{dt} \end{bmatrix} = \begin{bmatrix} 0 & -(1-D)/L \\ (1-D)/C(2D-1) & C(2D-1)/RC \end{bmatrix} \tag{8}$$

$$y(t) = (DC_1 + (1-D)C_2) \begin{bmatrix} i \\ u_c \end{bmatrix} \tag{9}$$

## 4.2 Perturb and Linearization

We know that low frequency and small ripple characteristic of the rectifier is satisfied, so the derivative of state vector in stable state equals to zero. According to that, we obtain that

$$X = -A^{-1}BU \tag{10}$$

$$A = DA_1 + (1-D)A_2, B = DB_1 + (1-D)B_2$$

Assume the small disturbance arises,

$$x = X + \hat{x}, y = Y + \hat{y}, u = U + \hat{u}, d = D + \hat{d} \tag{11}$$

$$\hat{x}(t) = A\hat{x}(t) + B\hat{u}(t) + [(A_1 - A_2)X + (B_1 - B_2)U]\hat{d}(t)$$

## 4.3 Transfer Function

So we get the transfer function of state variable and output variable expressed as

$$G_i(s) = \frac{\hat{i}}{\hat{u}_i} = \frac{1}{s^2 + \frac{s}{RC} + (1-D)^2/LC} * \left( \frac{s}{L} + \frac{1}{LRC} \right) \tag{12}$$

$$G_u(s) = \frac{\hat{u}_c}{\hat{u}_i} = \frac{1}{s^2 + \frac{s}{RC} + (1-D)^2/LC} * \left( \frac{1-D}{L} \right) \tag{13}$$

## 5. Closed Loop Control

The closed loop control consists of inner current loop and outer voltage loop. The inner loop needs a current controller and outer loop requires a voltage controller<sup>10</sup>. The overall block diagram of closed loop control for single phase rectifier is given as follows

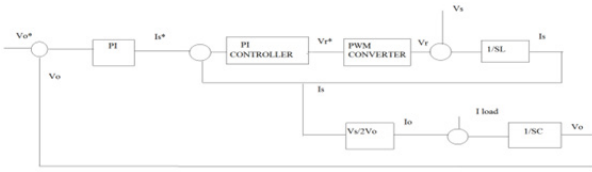


Figure 5. Closed loop block diagram.

The comparison of  $V_{ref}$  and  $V_0$  produce changes in capacitor voltage, change in capacitor voltage which in turn alter the output current, as output power is equal to input power change in output current will alter the input current. Hence the controller output is given as  $I_s^*$  (reference supply current) <sup>11</sup>. To match  $I_s^*$  and  $I_s$  it produce fundamental component of  $V_r$ .

If  $I_0$  matches  $I_{load}$ , no fluctuations in capacitor voltage, but in case not matches means it will produce fluctuations in capacitor voltage and as mentioned above all the parameters alter in order to match the fluctuations.

If we add a product block, multiplying with a sign term which is in phase with  $V_s$ , then it will give  $V_s$  and  $I_s$  in phase with each other, which means UPF in input side.

### 5.1 Inner Current Loop Control

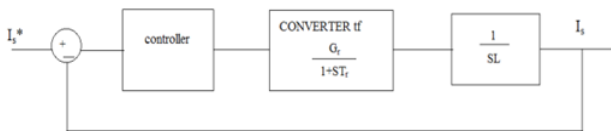


Figure 6. Inner current loop.

### 5.2 Converter

$G_r = V_r / M.I$   
 $V_r =$  Modulating voltage,  $M.I =$  Modulating Index  
 $T_r = 1/f_c$   
 $T_r =$  Time period,  $f_c =$  Carrier Frequency

### 5.3 Outer Voltage Loop

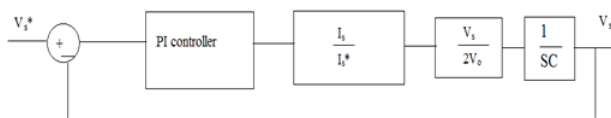


Figure 7. Outer loop.

### 5.4 Controller Design

Input current regulation in the converter is achieved by

adjusting the duty cycle. Generally three basic algorithm used are P, PI and PID. Here PI controller in the Inner current loop which regulate the input current, reduce peak over shoot and steady-state error. The PI consists of two basic modes that are proportional modes and integral modes. A proportional controller ( $k_p$ ) reduced settling time and reduced the error but not eliminated it. An integral controller ( $k_i$ ) will have the effect of eliminating the steady-state error. Limiter is used to control the duty cycle within the desirable band.

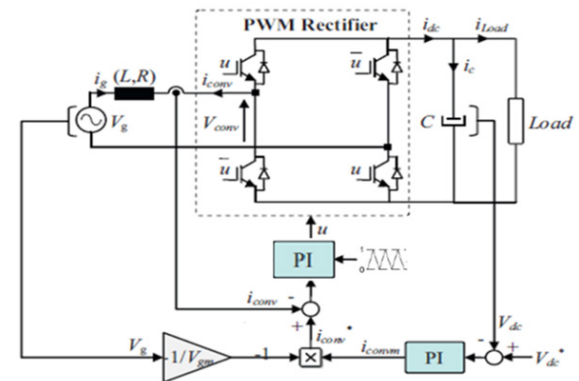
$$k_i = \frac{-D \sin \phi_d}{A_d \sin \beta}$$

$$K_p = \frac{-\sin(-\beta + \phi_d)}{A_d \sin \beta} - \frac{2k_i \cos \beta}{D}$$

$$S_d = -\xi \omega_n \pm j \omega_n \sqrt{1 - \xi^2} \text{ (Dominant Pole)}$$

$\xi =$  damping ratio  
 $\omega_n =$  natural frequency  
 $D = |S_d|$   
 $B = \text{Angle}(S_d)$   
 $A_d = |G[s_d]|$   
 $\Phi_d = \text{Angle}(|G[s_d]|)$

The physical model of closed loop control is given as follows



### 5.5 Simulation Results

Figure 8 shows the inner current loop control and Figure 9 shows the outer voltage loop control of a single phase PWM rectifier. Figure 10 shows the combination of inner current loop and outer voltage loop. Figure 11 shows the inner current loop settling for change in reference current. Figure 12 shows the outer current loop settling for different output voltages. Figure 13 the simulated waveform shows the inner current loop settles for different source voltage ( $V_s$ ). Figure 14 shows the outer voltage loop settles for different load currents. The closed

loop control using physical model is simulated with the  $V_{ref}$  is given as 400V. The simulation output representing the output voltage settles at 400V is given in the Figure 15 and the input current is stabilized using inner current loop which makes input current and voltage in phase, (UPF) is given in the Figure 16.

Here the PI controller is designed as  $K_p=.99724$ ,  $K_i=53.3$ ,  $I_{ref}=4A$ , here after the initial oscillations and peak over shoot, it settles with the given reference value. For outer voltage loop the PI controller is designed as  $K_p=.913$ ,  $K_i=2.27$ , The  $V_{ref}=400V$ .

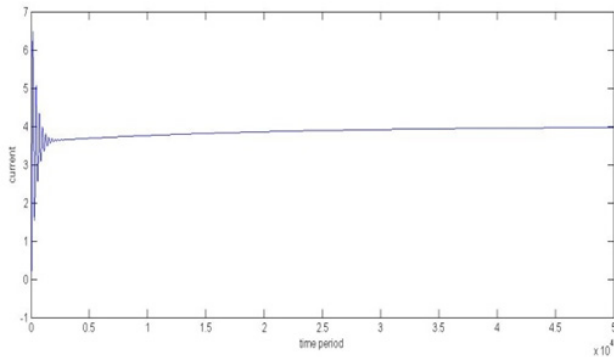


Figure 8. Inner Current Loop control.

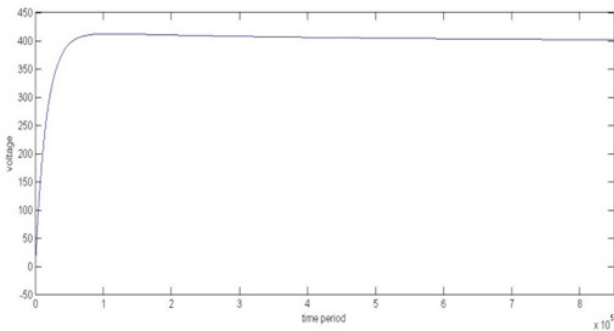


Figure 9. Outer voltage control.

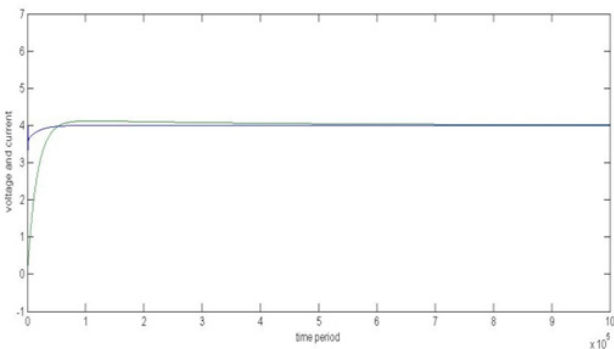


Figure 10. Combined loop.

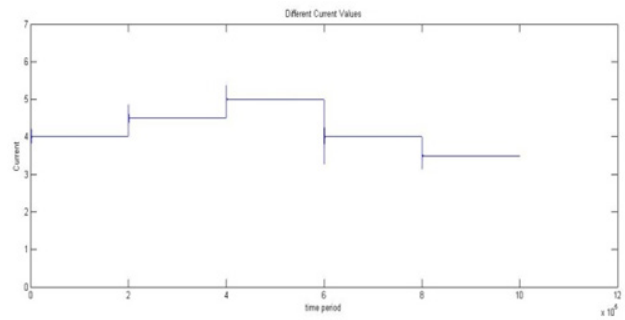


Figure 11. Different  $I_s^*$ .

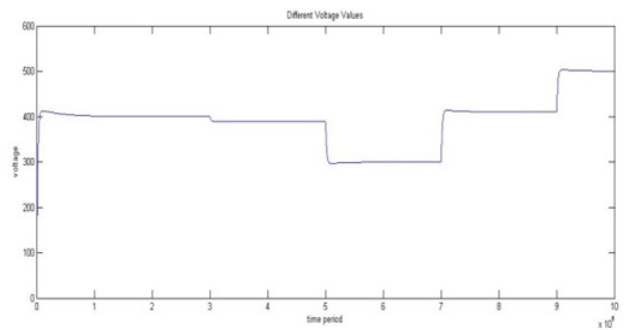


Figure 12. Different  $V_{ref}$ .

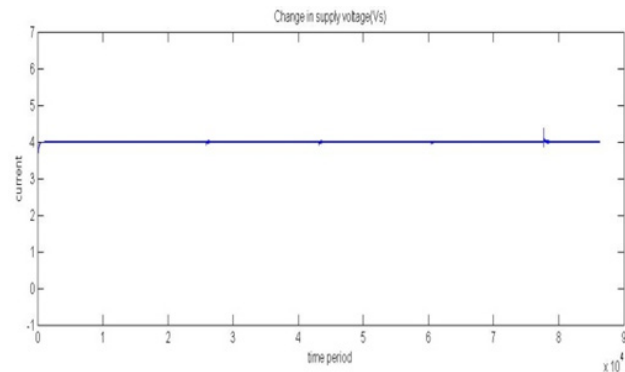


Figure 13. Change in  $V_s$  (current loop).

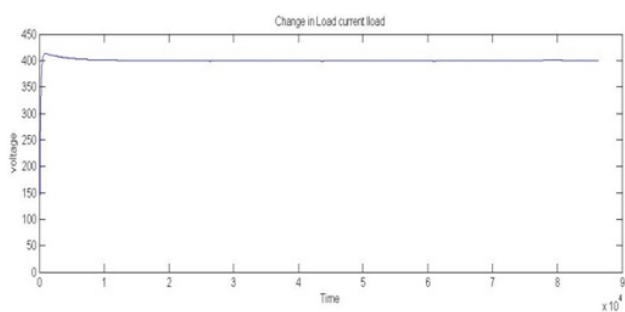


Figure 14. Change in Load current  $I_{load}$  (voltage loop).

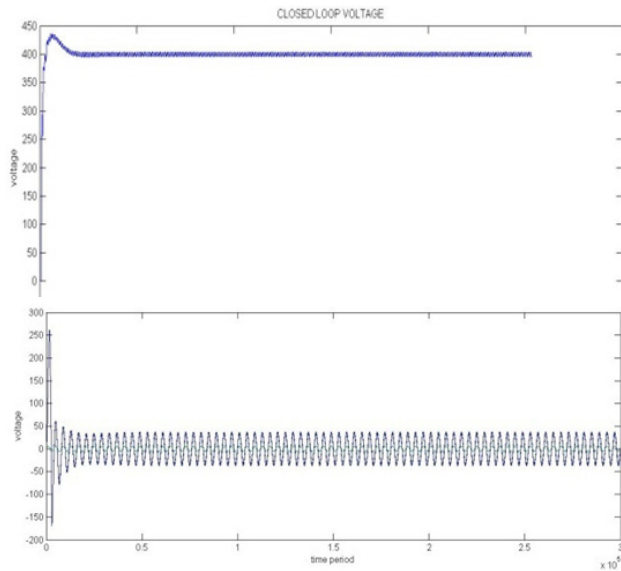


Figure 16. Closed Loop Input Voltage and current.

## 6. SISO Model for Three Phase PWM Rectifier

### 6.1 Introduction

A simple single-input–single-output model is constructed by separating the d-axis and the q-axis dynamics through appropriate nonlinear feed forward decoupling while maintaining nearly unity power factor operation. The model exhibits a close similarity to a dc–dc boost converter under both large-signal and small-signal operating conditions. This makes it possible to extend the system analysis and control design techniques of dc–dc converters to the three-phase PWM rectifier also. The validity of the proposed model has been verified in the frequency domain under open-loop operation of the PWM rectifier. The usefulness of the model is further demonstrated through closed-loop operation of the rectifier with both voltage mode and inner-current-loop-based schemes.

### 6.2 Three Phase PWM Rectifier

Over the past several years, considerable research work has been carried out on the control of ac-to-dc Pulse Width Modulation (PWM) rectifiers, since these converters possess many desirable features such as sinusoidal line currents at a required power factor, a nearly constant dc output voltage, and bidirectional power delivery

capability. As the filter capacitor required is generally small under balanced supply voltage conditions, it may also be believed that these converters can offer excellent dynamic response of the dc output voltage.

Control of three-phase PWM rectifiers in the d–q Synchronously Rotating Frame (SRF) has been developed from field oriented control techniques for ac drives in early 1980s. Normally, the control objectives of a PWM rectifier are to regulate the dc output voltage on the dc side, achieve Unity Power Factor (UPF) operation on the ac side, and also to achieve fast dynamic response to line and load disturbances. A state-space averaged model has been proposed for the three-phase PWM rectifier in the d–q SRF. However, the model, though accurate, does not give sufficient insight into the controller design and behavior of the three-phase PWM rectifier system due to its complex Multi Input–Multi Output (MIMO) nonlinear structure and the presence of a non minimum phase feature. Due to this, designing a proper controller for such a converter has been generally a challenging task. The SISO model equation has been derived in <sup>1</sup>. It deals with the closed loop control of three phase rectifier with SISO model.

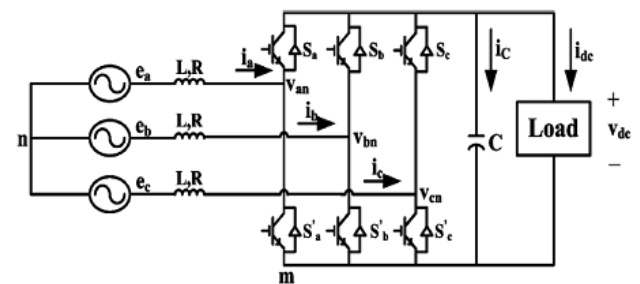


Figure 17. Three Phase PWM Rectifier.

### 6.3 Equivalent Circuit for SISO Model

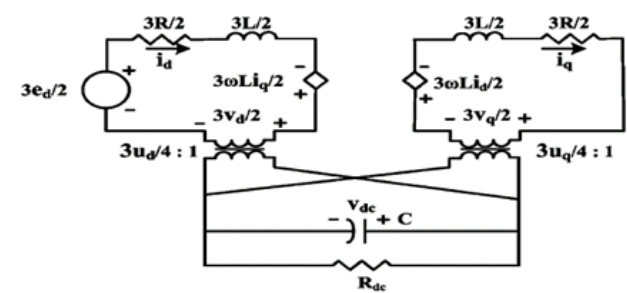


Figure 18. Equivalent circuit in SRF.

### 6.4 Non Linear Feed Forward Decoupling Controller

In Figure 19 the coupling terms between the d-axis and the q-axis are represented by the two current-controlled dependent voltage sources. Decoupling may be achieved, if the effects of these two voltage sources are nullified by appropriately adjusting the control inputs  $v_d$  and  $v_q$ .

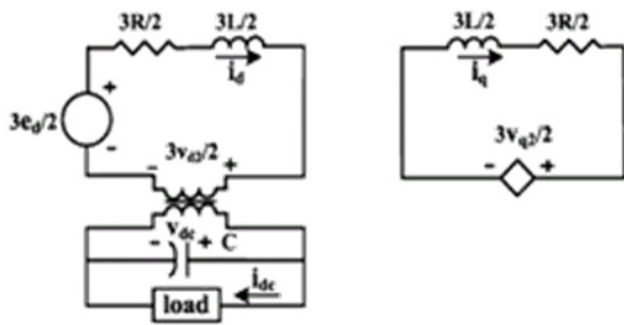


Figure 19. Equivalent circuit in SRF after decoupling q-axis.

### 6.5 Closed Loop Control

It is well known that the output performance of a single-phase power factor correction unit is limited by the slow response of the bulky capacitor. This drawback is overcome by a three-phase PWM rectifier as it successfully gets rid of the line-frequency related ripple on the dc side. This allows ripple-free output voltage operation to be achieved even with a small filter capacitor. Here,  $F_i(s)$  is the control to- d-axis current transfer function given in <sup>1</sup>. In designing a multiloop controller, one first designs the inner loop. Here the controller used is PI controller

Once the current loop is closed, the converter can be treated as a new open-loop plant with transfer function  $F_{vi}(s)$  given in <sup>1</sup>. Here this acts as an outer voltage loop model.

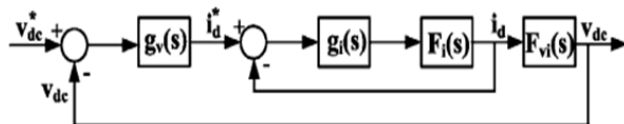


Figure 20. Closed loop control.

### 6.6 Simulation Results

Figure 21 shows the inner current loop design with a PI

controller and Figure 22 shows the outer voltage loop control.

Here the closed loop is designed for input voltage  $E_d=230V$ ,  $L$  can be designed as  $.003H$  and  $C=.000136F$ . The controller used is PI controller and  $K_p$  proportional constant is kept unity, while  $K_i$  integral constant is designed as 53.3 in Time domain to reduce the steady state error

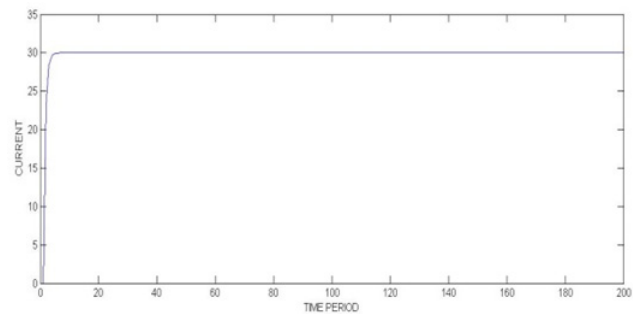


Figure 21. Inner current control for three phase PWM rectifier.

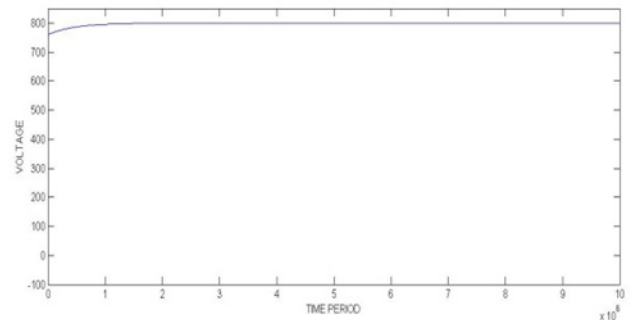


Figure 22. Outer voltage control for three phase PWM rectifier.

## 7. Conclusion

The physical model and mathematical model are designed for single phase rectifier. The closed loop control for single phase PWM rectifier with PI controllers also designed using mathematical model and verified with physical model. SISO model for three phase rectifier and closed loop control are designed for a three phase rectifier. Simulation is done using MATLAB and the simulation results are shown. In future the mathematical SISO model can be simulated.

## 8. References

1. Yin B, Oruganti R. A Simple Single-Input-Single-Output (SISO) Model for a Three-Phase PWM Rectifier, *IEEE Trans Ind Electron*. 2009 Nov; 24(03).
2. Anbuselvi S, Rebecca J. A comparative study on the biodegradation of coir waste by three different species of Marine cyanobacteria, ISSN: 1815-932x, *Journal of Applied Sciences Research*. 2009; 5(12):2369-74.
3. Yin B, Oruganti R, Panda SK, Bhat AKS. Experimental verification of a dual single-input single-output (SISO) model of a three phase boost-type PWM rectifier, in *Proc 31st IEEE Conf Ind Electron Soc*; 2005. P. 1030-5.
4. Hiti S, Boroyevich D, Cuadros C. Small-signal modelling and control of three-phase PWM converters, in *Proc Ind Appl Soc Annu Meeting*. 1994 Oct; 2:1143-50.
5. Bharatwaj RS, Vijaya K, Rajaram P. A descriptive study of knowledge, attitude and practice with regard to voluntary blood donation among medical undergraduate students in Pondicherry, India, ISSN : 0973 - 709X, *Journal of Clinical and Diagnostic Research*. 2012; 6(S4):602-4.
6. Yin B, Oruganti R, Panda SK, Bhat AKS. Performance comparison of voltage mode control and current mode control of a three-phase PWM rectifier based on dual SISO model, in *Proc 32nd IEEE Conf Ind Electron Soc*, Paris, France; 2006 Nov. p. 1908-14.
7. Raj MS, Saravanan T, Srinivasan V. A modified direct torque control of induction motor using space vector modulation technique, ISSN: 1990-9233, *Middle - East Journal of Scientific Research*. 2014; 20(11):1572-4.
8. Wei J. Analysis and Design of A Single-Phase PWM Rectifier Based On the Small Signal Model 978-1-4244-4994-1/09 ©2009.
9. Rajasulochana P, Krishnamoorthy P, Dhamotharan R. An Investigation on the evaluation of heavy metals in *Kappaphycus alvarezii*, ISSN: 0975 - 7384, *Journal of Chemical and Pharmaceutical Research*, 2012; 4(6):3224-8.
10. Erickson RB. *Fundamentals of Power electronics*.
11. Jasmine MIF, Yezdani AA, Tajir F, Venu RM. Analysis of stress in bone and micro implants during en-masse retraction of maxillary and mandibular anterior teeth with different insertion angulations: A 3-dimensional finite element analysis study, ISSN : 0889-5406, *American Journal of Orthodontics and Dentofacial Orthopedics*. 2012; 141(1):71-80.